Amine-Functionalized Porous Silicas as Adsorbents for Aldehyde Abatement

Akihiro Nomura and Christopher W. Jones*

School of Chemical & Biomolecular Engineering, Georgia Institute of Technology, 311 Ferst Drive, Atlanta, Georgia 30332-0100, United States

Ⓢ Supporting Information

ABSTRACT: A series of aminopropyl-functionalized silicas containing of primary, secondary, or tertiary amines is fabricated via silane-grafting on mesoporous SBA-15 silica and the utility of each material in the adsorption of volatile aldehydes from air is systematically assessed. A particular emphasis is placed on low-molecular-weight aldehydes such as formaldehyde and acetaldehyde, which are highly problematic volatile organic compound (VOC) pollutants. The adsorption tests demonstrate that the aminosilica materials with primary amines most effectively adsorbed formaldehyde with an adsorption capacity of 1.4 $mmol_{HCHO}$ g^{-1}, whereas the aminosilica containing secondary amines showed lower adsorption capacity (0.80 $mmol_{HCHO}$ g^{-1}) and the aminosilica containing tertiary amines adsorbed a negligible amount of formaldehyde. The primary amine containing silica also successfully abated higher aldehyde VOC pollutants, including acetaldehyde, hexanal, and benzaldehyde, by effectively adsorbing them. The adsorption mechanism is investigated by ^{13}C CP MAS solid-state NMR and FT-Raman spectroscopy, and it is demonstrated that the aldehydes are chemically attached to the surface of aminosilica in the form of imines and hemiaminals. The high aldehyde adsorption capacities of the primary aminosilicas in this study demonstrate the utility of amine-functionalized silica materials for reduction of gaseous aldehydes.

KEYWORDS: aminosilica, aldehyde, adsorption, mesoporous silica, air qualification, volatile organic compound (VOC)
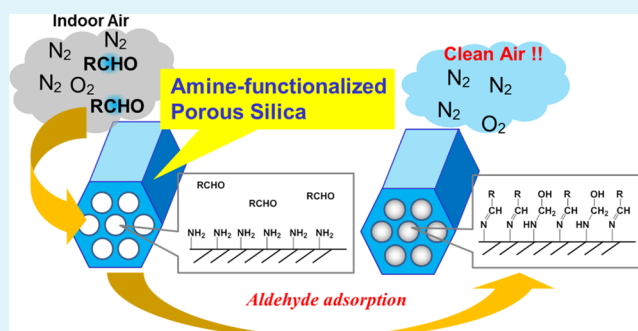
INTRODUCTION

Because air quality is an area of emerging importance for human health, the development of commercially viable materials that can reduce volatile organic compounds (VOCs) is attracting increasing research interest.[1−5] Among several common VOCs, airborne formaldehyde is the most targeted compound in the view of its toxicity and ubiquitous use in resins and adhesives. Formaldehyde is a carcinogen and allergen, and it can intensely irritate the eyes and mucous membranes.

To this end, several materials have been reported for the purpose of gaseous formaldehyde abatement. There are two main strategies for removing formaldehyde from air; one is catalytic removal by combusting formaldehyde into carbon dioxide and water, and the other is adsorptive removal of airborne formaldehyde. There are many reports on catalytic removal methods, clarifying approaches for the efficient conversion of formaldehyde into carbon dioxide gas.[6−10] However, this method still faces problems for practical formaldehyde abatement due to the use of expensive precious metals (palladium or platinum) and the potential need for thermal energy. Photocatalytic combustion of airborne formaldehyde has also been reported, but the poor availability of UV light sources in some scenarios can prove problematic for air qualification methodologies.[11−14]

Whereas research targeting formaldehyde abatement catalysts has targeted materials free of precious metals, the adsorptive removal method has focused on developing amine-functionalized materials that efficiently and strongly bind aldehydes. Aldehydes can be effectively captured on amine-modified surfaces via covalent amine and aldehyde coupling reactions, targeting formation of imines.[15] Since Gesser first disclosed use of a polymeric amine coating of poly(ethyleneimine) on various materials to capture aldehyde air pollutants,[16] several amine-functionalized materials have been developed specifically targeting airborne formaldehyde removal.[17−19] The structure of the amine moieties and the site density of the amines are both important to the development of highly efficient formaldehyde sinks. This adsorptive removal method may be a much more practical way for air purification, as the adsorption occurs at ambient conditions, and is suitable to a wider array of conditions, as no heat or UV light is needed. To this end, many methods of applying amine-functionalized materials for air purification have been disclosed in several patents.[16,20−31] However, the adsorption mechanism has been less discussed.

Tanada et al. demonstrated that aminated activated carbon materials with higher amine loadings showed higher adsorption capacities for formaldehyde from aqueous solution, linking the amine loading directly to uptake capacity.[32] Later, Boonamnuayvitaya et al. synthesized amine-functionalized mesoporous silica materials via co-condensation of tetraethyl orthosilicate (TEOS) and N-(2-aminoethyl)-3-aminopropyltrimethoxysilane and found that there was an optimal amine-loading for maximizing gaseous formaldehyde adsorption. Specifically, they demonstrated that medium loading aminosilica exhibited the highest formaldehyde adsorption ability compared to lower or higher amine loaded materials.[33] Similar results have been shown in our lab for CO_2 adsorption, whereby higher amine loadings led to steric constraints that made some amine sites inaccessible to gas phase species on practical time scales.[34] Drese et al. functionalized the surface of mesoporous silica with several aminosilanes and demonstrated the materials in the selective removal of aldehydes from bio-oils, and they reported primary amine moieties were most effective for aldehydes trapping.[35] Very recently, Gibson and Patwardhan et al. reported amine-functionalized silica as an airborne formaldehyde gas adsorbent at an air contaminant level of 1 ppm, and found amine-functionalized surfaces to be highly effective for trapping formaldehyde. However, the correlation between the adsorption ability and mechanism is still unclear.[36] These previous works strongly indicate that the effective design of the support porosity coupled with the use of specific molecular amine structures can be used to achieve further improved aldehyde adsorbing materials.

In this work, we demonstrate that amine-functionalized porous silica materials are excellent candidate materials for gaseous aldehyde abatement, having high adsorption capacities for formaldehydes as well as several higher aldehydes. Mesoporous SBA-15 silica was used as the substrate for surface tethering of a variety of aminosilanes, including silanes containing primary (APS), secondary (MAPS), and tertiary aminosilanes (DMAPS), respectively.[37] We demonstrate that the primary amine treated silica is particularly effective for capturing aldehydes, probe the adsorption mechanism in detail using FT-Raman spectroscopy and ^{13}C CP-MAS solid state NMR with ^{13}C labeled aldehydes. Our work demonstrates how air purification materials may be designed for better performance. Thus improved air quality could be achieved thru their incorporation into air purifying systems, filters, or coatings.

■ EXPERIMENTAL SECTION

Materials. The following chemicals were used as received from the suppliers: tetraethyl orthosilicate (TEOS, 98%, Sigma-Aldrich), pluronic EO-PO-EO triblock copolymer (P123, Sigma-Aldrich) hydrochloric acid (HCl, 37% fuming, EMD Millipore), 3-aminopropyl-trimethoxysilane (APS, >95%, Gelest), N-methylaminopropyl-trimethoxysilane (MAPS, >95%, Gelest), N,N-dimethylaminopropyl-trimethoxysilane (DMAPS, 96%, Sigma-Aldrich), propyltrimethoxysilane (nPS, >98%, Alfa Aesar), and 3-chloropropyl-trimethoxysilane (ClPS, >97%, Alfa Aesar), formaldehyde (36.5% aqueous solution, BDH), acetaldehyde (98.5%, Alfa Aesar), hexanal (98%, Alfa Aesar), benzaldehyde (99%+, Aldrich), acetone (99.5%, BDH), propylamine (99+%, Acros Organics). Acetonitrile (HPLC grade, EMD) and water (HPLC grade, J. T. Baker) were used as HPLC eluent solvent. ^{13}C labeled formaldehyde ($H^{13}CHO$) and acetaldehyde ($^{13}CH_3^{13}CHO$) were obtained from CIL Inc. UHP grade dry air gas (water and carbon dioxide (CO_2) free air, synthetic blend of nitrogen and oxygen) was obtained from Airgas Inc., and 1% CO_2 in helium was purchased from Matheson Tri-Gas. The commercial mesostructured silica gel PD09024 was obtained from the PQ Corporation. Sorbent tubes

filled with 2,4-dinitrophenylhydrazine (DNPH) coated silica gel were purchased from SKC Inc. (cat. 226−119) for the determination of aldehyde gas concentrations. Standard acetonitrile solutions of formaldehyde-DNPH, acetaldehyde-DNPH, hexanal-DNPH, benzaldehyde-DNPH, and acetone-DNPH were purchased from Sigma-Aldrich for HPLC peak calibration. All other reagents and solvents were general laboratory grade and used as received from the commercial source.

Synthesis. Mesoporous silica SBA-15 was used as the amine-functionalized silica support for these studies and was synthesized following a procedure in the literature.[35,38] The synthetic procedure began with dissolving P123 (12 g) in a solution 320 g of deionized water and 60 g of HCl at room temperature. After complete dissolution of P123, the solution was vigorously stirred at 40 °C for 2 h and then 23.1 of TEOS was added to the solution and stirred at 40 °C overnight. The solution was heated to 100 °C and kept stirring overnight. The reaction mixture was quenched with deionized water (200 g) before the resulting solid was filtered, washed with copious amounts of deionized water, dried overnight at 75 °C, and then calcined in air at 550 °C with a 1.2 °C min^{-1} ramp. Approximately 6.6 g of SBA-15 silica was collected with this method.

Aminosilane-functionalized SBA-15 was prepared according to a previously published procedure.[35,39] In a typical synthesis, the aminosilane (ca. 22 mmol, in the case of APS) was added to SBA-15 (2.0 g) dispersed in toluene (ca. 100 mL). The mixture was stirred at room temperature for 24 h. The solid amine-functionalized silica was filtered, washed with copious toluene, and dried overnight at 75 °C. The same procedure was followed for MAPS and DMAPS treated silicas, including propyltrimethoxysilane (nPS) and 3-chloropropyl-trimethoxysilane (ClPS) treated silicas.

Characterization of Materials. Thermogravimetric analysis was performed on a Netzsch STA409. Samples were heated from r. t. to 900 °C at a rate of 10 °C min^{-1} under a stream of nitrogen and air. The organic loading was determined by weight loss between 150 and 800 °C, assuming two methoxy linkages from the silane were hydrolyzed to link the silane to the surface. FT Raman spectra were obtained on a Bruker Vertex 80v optical bench with a RAMII Raman module at a resolution of 4 cm^{-1}. Nitrogen physisorption analysis was performed on a Micromeritics Tristar II at 77 K, with surface area determined by the Brunauer−Emmett−Teller (BET) method.[40] Pore volumes and pore diameters of bare SBA-15 silica supports and silane-treated silicas were calculated using the BdB-FHH method.[41,42] ^{13}C CP-MAS solid state NMR was performed on a Bruker DSX-300 spectrometer. The samples were spun at a frequency of 10 kHz. ^{13}C and ^1H solution NMR spectra were recorded on a Bruker AMX 400 (400 MHz).

Airborne Aldehyde Abatement Tests. Before aldehyde abatement tests, all adsorbent samples were dried under vacuum overnight at ca. 100 °C to remove physisorbed water and carbon dioxide. The silica (ca. 15 mg) was enclosed in a gas sampling bag (Tedlar, 10 L, Restek Corp.) before 8 L of dry air was added to fill the gas sampling bag. For the formaldehyde abatement test, 10 μL of aqueous solution of formaldehyde (10 wt %) was injected into the gas sampling bag by a microsyringe to set the initial formaldehyde gas concentration inside the gas sampling bag to ca. 100 ppm, and then the system was equilibrated at room temperature. For the acetaldehyde abatement test, 10 μL of acetonitrile solution of acetaldehyde (20 wt %) was injected to set the gas concentration at ca. 100 ppm. The same procedure was followed for the abatement tests using other higher aldehydes and acetone, except that the exact volumes of neat liquids were injected to set their initial gas concentrations as ca. 100 ppm.

Aldehyde gas concentrations were determined by following the US EPA method TO-11/IP-6A. In a typical procedure, 500 mL of the gas content was extracted by gas sampling pump (Grab Air Sample Pump, SKC Inc.) through a DNPH sorbent tube. The gas flow rate (typically 200 − 250 mL min^{-1}) was measured each sampling time with a mass flow meter (FMA1814, Omega Engineering Inc.) to determine the suction time securing a fixed volume (500 mL) of extracted gas. The sorbent section was then placed in a 2 drum vial and 2.5 mL of acetonitrile was added. The vial was periodically shaken to extract the

DNPH-aldehyde adduct, and the extract was analyzed using an HPLC system from Shimadzu, consisting of ODS silica gel columns (Chromegabond WR C18 5 μm 120 Å, 15 cm × 4.6 mm, ES Industries) and a UV−vis detector (SPD-10AVP, Shimadzu Corp.). The separation was conducted at 40 °C, typically with the mobile phase of 60/40 acetonitorile/water mixture at a flow rate of 1.0 mL/min. The UV response was monitored at the wavelength of 360 nm. The reduction of the aldehyde gas concentration inside the gas sampling bag was determined by the peak area ratio of the DNPH-aldehyde adduct with that of the initial gas sampling with no adsorbent (blank gas sampling bag having ca. 100 ppm aldehydes), and its exact molar concentration was determined by calibrating the peak area with DNPH-aldehyde standard solutions.

The adsorption capacity, q, and amine efficiency, μ, are to evaluate the adsorption abilities of aminosilicas in this study. The adsorption capacity q, which is defined as molar quantity of adsorbed gas per unit weight of aminosilica adsorbent, was calculated using the assumption that all of the abated gas was trapped into the silica adsorbent. The amine efficiency, μ, which is defined as the molar ratio of adsorbed gas to amine moiety, was calculated by dividing q by the amine loading.

■ RESULT AND DISCUSSION

Airborne Aldehydes Adsorption. Though it is known that amine-treated materials dramatically enhance adsorption of airborne aldehydes,[18,32,33,35,36] an understanding of the role of amine structure on the adsorption capacity and mechanism has not been developed. For a systematic study of aldehyde vapor adsorption by amine-functionalized materials, three aminosilica adsorbents were prepared using silane chemistry to graft mesoporous silica SBA-15 with primary, secondary, and tertiary aminopropylsilanes of APS, MAPS, and DMAPS, respectively. The SBA-15 silica support has a large surface area, large pore volume, and large pore diameter,[43] which allow for fast diffusion of gaseous or vapor adsorbates to adsorption sites. S-AP, S-MAP, S-DMAP denote the corresponding samples for the three aminosilane-treated SBA-15 silicas. As all of the amines are structurally similar, being linked to the surface via propyl groups, systematic comparison of amine reactivity of the different types of amine sites is possible. Silica materials functionalized with n-propyl and 3-chloropropyl groups (nPS and ClPS) were also prepared on SBA-15 (S-nP and S-ClP) so that the contribution of an unfunctionalized alkyl chain and or a nonamine-containing polar functional group could be assessed. A similar approach has been used previously by our group and others for examining the effect of structural differences on carbon dioxide gas adsorption.[37,44−46] Table 1 shows the characteristics of the silica adsorbents used in this study (TGA

data are given and nitrogen adsorption−desorption isotherms are available in the Supporting Information). Although the BET surface area of SBA-15 decreased by about half after the silane-coupling reactions, the obtained silica adsorbents had nearly the same amine loading density, surface area, and pore volume, so that direct comparisons could be made between adsorption characteristics over the various solids.

Formaldehyde abatement was conducted with those functionalized silicas. At first, abatement tests at 10 ppm formaldehyde concentrations were completed. However, the airborne aldehyde concentrations dropped to undetectable concentrations (∼0 ppm) within an hour with the S-AP adsorbent and the total adsorption capacity could not be evaluated (see the Supporting Information). Thus, we chose to conduct the abatement tests with higher formaldehyde concentrations of 100 ppm to systematically evaluate the adsorption capacities of the aminosilica adsorbents used in this study. Although this concentration is much higher than the realistic atmospheric air contaminant concentrations (i.e., ca. 1 ppm), this study demonstrates the adsorption potential of aminosilicas as aldehyde adsorbents under conditions that allow accurate quantification of adsorption capacities and characterization of adsorbed intermediates.

Panels a and b in Figure 1 show the results of the ca. 100 ppm formaldehyde abatement tests. The gas sampling bag with
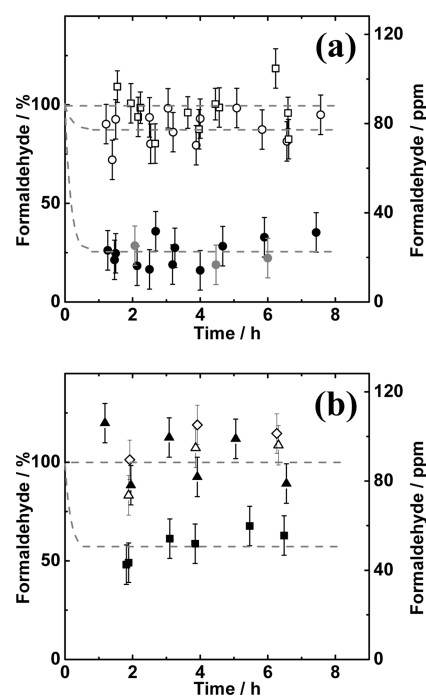

Figure 1. Formaldehyde concentrations inside the gas sampling bags plotted against elapsed time after its injection. (a) Each data point denotes gas sampling bags with: no adsorbent (□), SBA-15 (○), S-AP (●), and S-AP under 1% CO_2 atmosphere (gray dot). (b) Each data point denotes the gas sampling bags with: S-MAP (■), S-DMAP (▲), S-nP (◇), and S-ClP (△).

Table 1. Physical Characteristics of Functionalized Mesoporous Silicas in This Study

	amine loading ($mmol_N$ g^{-1})	organic content (%)	pore diameter D_p (nm)	pore volume V_p (cm^3 g^{-1})	surface area S_{BET} (m^2 g^{-1})
SBA-15	n/a	n/a	7.6	1.14	922
S-AP	1.9	14	7.0	0.72	422
S-MAP	1.8	16	6.6	0.69	401
S-DMAP	1.7	17	6.5	0.68	392
S-nP[a]	1.4[a]	8.0	7.5	0.98	676
S-ClP[b]	1.9[b]	18	7.1	0.77	546
PD09024	n/a	n/a	17	1.03	364
P-AP	0.97	7.1	17	0.86	289

[a]Propyl chain loading density was listed. [b]Chloride loading density was listed.

no silica adsorbent maintained the initial formaldehyde concentration (88 ppm), showing that no significant leakage of formaldehyde gas occurred within the examined time period (Figure 1 (a)). The initial formaldehyde concentration of 88 ppm was slightly less than the calculated volume of form-aldehyde needed to set its initial concentration at 100 ppm,

showing that not all of injected formaldehyde was successfully vaporized inside the gas sampling bag. This may be due to the formation of nonvolatile formaldehyde polymers (polyacetals) within the injected formaldehyde aqueous solution. Bare SBA-15 silica slightly decreased the gas concentration to 78 ppm, 88% of its initial concentration, suggesting that formaldehyde was partially adsorbed onto the silica surface. Though it is not clear in this case the precise surface interactions that captured the formaldehyde, surface silanols on silica are presumed to interact with the carbonyl function of the aldehyde, which could promote aldehyde adsorption.[47] The high surface area of SBA-15 undoubtedly also promotes this adsorption, by providing a large number of adsorption sites. On the other hand, the gas sampling bag with the S-AP primary aminosilica adsorbent dramatically decreased the formaldehyde concentration to 22 ppm (25% of starting concentration) within an hour. This clearly indicates that surface amine moieties play a crucial role in the formaldehyde adsorption, and supports the notion that S-AP may be a valuable aldehyde abatement material. It has been reported that such aminosilica materials are carbon dioxide (CO_2) adsorbents that can remove CO_2 efficiently from ambient air.[48] To probe whether CO_2 may outcompete formaldehyde for amines sites, we carried out a formaldehyde abatement test under a 1% CO_2 atmosphere (air is about 400 ppm CO_2, or 0.04%). The results shown in Figure 1 demonstrate that even CO_2 concentrations 25 fold higher than that found in ambient air do not result in substantially reduced aldehyde adsorption.

While the S-AP sample proved to be quite useful, the adsorption of formaldehyde became less significant when the secondary amine containing S-MAP was used, decreasing the formaldehyde concentration to 51 ppm, or 58% of the initial value. The S-DMAP sampled proved even worse, showing negligible formaldehyde adsorption (Figure 1b). This suggests that the primary amine group shows the highest utility, as expected, assuming imine formation as the primary adsorption mode. The S-nP and S-ClP silicas did not decrease the formaldehyde concentration at all, indicating that propyl chain or propyl halides have no effect on formaldehyde adsorption, or adversely, they were ill-designed for the purpose of form-aldehyde adsorption by removing the surface silanols that presumably allowed the bare silica to capture some form-aldehyde. These control experiments clearly show that amines are the active moieties that remove the aldehydes.

Table 2 shows the tabulated results of the formaldehyde abatement tests. The adsorption capacity, q, was derived with an assumption that all of the decreased formaldehyde was trapped into the silica adsorbent. The q of S-AP (1.4 $mmol_{HCHO}$ g^{-1}) is high, similar to the values observed for aminosilicas when used as CO_2 adsorbents, and can be understood as nearly the maximum possible value for this S-AP silica adsorbent, by referring to the aldehyde capturing efficiency. The capturing efficiency, μ, of S-AP, defined as the molar ratio of adsorbed formaldehyde to amine nitrogens, was 0.76. This value of close to unity indicates that nearly all of amine moieties were consumed during the aldehyde adsorption. Thus, if the formaldehyde reacted with the primary amine in a one to one ratio, then the q value could be further improved if one could increase the primary amine density while maintaining good site accessibility.[34] The μ of S-MAP was about half the value of the μ of S-AP, and the μ of S-DMAP was zero, confirming the particular activity of primary amines for capturing formaldehyde.

Table 2. Formaldehyde Adsorption Capacities, q, and Amine Efficiencies, μ

	q ($mmol_{HCHO}$ g^{-1})	μ ($mmol_{HCHO}$ $mmol_N^{-1}$)
SBA-15	0.22	n/a
S-AP	1.4	0.76
S-AP[a]	1.5[a]	0.78[a]
S-MAP	0.80	0.43
S-DMAP	0.0	0.0
S-nP	0.0	0.0[b]
S-ClP	0.0	0.0[c]
PD09024	0.41	n/a
P-AP	1.2	1.2 (0.82[d])

[a]Adsorption data corrected under 1% CO_2 in helium atmosphere. [b]Molar ratio of captured formaldehyde and propyl chain. [c]Molar ratio of captured formaldehyde and chloride. [d]The capturing efficiency was derived by subtracting the adsorption capacity q of bare PD09024.

As primary amines were found to be most effective for formaldehyde abatement, APS was also treated on a commercially available silica, PD09024, from the PQ Corporation. This PD09024 silica has a mesocellular foam (MCF) type of pore structure and its characteristics are given in Table 1. P-AP is the nomenclature used to denote the APS-treated PD09024 silica sample. Figure 2 shows the results of
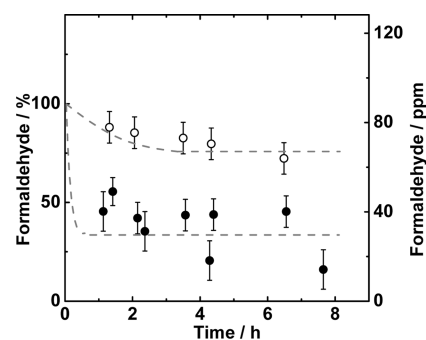

Figure 2. Formaldehyde concentrations inside the gas sampling bags with PD09024 (○) and P-AP (●) plotted against elapsed time after its injection.

formaldehyde abatements with bare PD09024 and P-AP silicas, and their numerical data are tabulated in Table 2. Both the bare PD09024 and P-AP silicas reduced the formaldehyde concentration, though they took about 1 h longer to reach a constant formaldehyde concentration than the abatement with bare SBA-15 and S-AP silicas. This slower adsorption may be associated with larger particle size of PD09024 silica (average particle size of 6.5 μm) compared to SBA-15 (<1 μm from SEM image, see the Supporting Information), requiring longer time to diffuse the adsorbate gas into the center of the particle. However, it still can be said that PD09024 and especially amine treated P-AP are quite effective for formaldehyde abatement. The q of P-AP was as high as that of S-AP, but the P-AP sample had about half the amine loading of S-AP, a reduction proportional to the respective support surface areas. Therefore, the μ value of P-AP (1.2) was greater than unity. However, the bare PD09024 silica also showed much higher formaldehyde adsorption relative to SBA-15, which likely increases the base adsorption capacity of P-AP. If one recalculates the μ value of P-AP by subtracting the adsorption capacity of PD09024, the μ value becomes 0.82, similar to that of the SBA-15 supported

5572

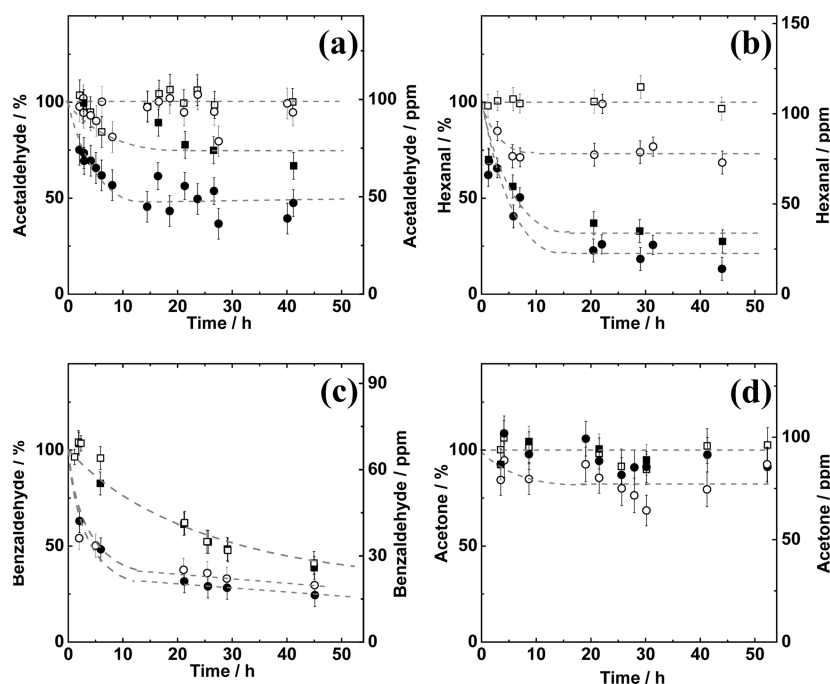dx.doi.org/10.1021/am400810s | ACS Appl. Mater. Interfaces 2013, 5, 5569–5577

Figure 3. (a) Acetaldehyde, (b) hexanal, (c) benzaldehyde, and (d) acetone gaseous concentrations inside the gas sampling bags plotted against elapsed time after its injection. Each data point denotes the gas sampling bags with: no adsorbent (□), SBA-15 (○), S-AP (●), and S-MAP (■).

Table 3. Adsorption Capacities, q, and Amine Efficiencies, μ, of SBA-15, S-AP, and S-MAP for Airborne Acetaldehyde, Hexanal, and Acetone Gases

	acetaldehyde		hexanal		acetone	
	q (mmol g^{-1})	μ (mmol mmol$_N^{-1}$)	q (mmol g^{-1})	μ (mmol mmol$_N^{-1}$)	q (mmol g^{-1})	μ (mmol mmol$_N^{-1}$)
SBA-15	0.08	n/a	0.50	n/a	0.35	n/a
S-AP	1.1	0.56	1.8	0.96	0.11	0.06
S-MAP	0.48	0.26	1.5	0.84	0.04	0.02

sample, thereby supporting this hypothesis. The reason for the increased formaldehyde adsorption of PD09024 is not clear, but may be associated with some metal or other impurities present in the commercial PD09024 silica.[49] In any case, this success using a commercial silica as the amine substrate for formaldehyde adsorption shows that well-defined, expensive supports such as SBA-15 are not needed for this application.

The driving force for the formaldehyde adsorption by amine-functionalized silica is the chemical reaction between the carbonyl function and the amine, as discussed below. The reaction is not limited to airborne formaldehyde, and should also be applicable to other airborne aldehydes and ketones. To this end, we carried out VOC abatement tests using acetaldehyde, hexanal, benzaldehyde, and acetone, which are also irritant VOCs or appropriate test molecules. Figure 3 shows the results of the VOC abatement tests, and their tabulated data are summarized in Table 3. Adsorption of these molecules required much longer times, 10 h or more, to reach equivalent surface loadings as observed for formaldehyde, probably due to two factors, the lower volatility and the larger molecular size of the adsorbates, leading to lower diffusion rates through the silica, the latter of which likely plays a more important role. However, the primary S-AP aminosilica was shown to be effective for the abatement all of these VOCs except for acetone. The adsorption behavior of acetaldehyde and hexanal can be discussed in the same way as with that of formaldehyde (Figure 3a, b), because the q increased from the bare SBA-15 to S-MAP and finally to S-AP. The initial gas concentrations of acetaldehyde and hexanal for their abatement tests were 99 and 106 ppm, respectively, close to the 100 ppm targeted injection concentration. Hexanal was more effectively abated by all the silica adsorbates including SBA-15, S-MAP, and S-AP, compared to formaldehyde and acetaldehyde. Water and acetonitrile were added also present in the injected liquids in the case of formaldehyde and acetaldehyde, respectively, which might have somehow hindered their adsorption relative to hexanal. Benzaldehyde showed self-reduction behavior, as the initial gas concentration of 67 ppm was much less than the intended concentration of 100 ppm and the gas concentration within the gas sampling bag with no adsorbate silica clearly decayed along with time (Figure 3c). This self-reduction results from aerobic auto-oxidation, in which aldehydes are oxidized to corresponding carboxylic acids (benzoic acid, in the case of benzaldehyde) under the presence of oxygen in the air.[50] As the aerobic auto-oxidation proceeds via a radical process, benzaldehyde is much more affected by the oxidation than the other aldehydes here, because of the presence of phenyl group that stabilizes the benzoyl radical intermediate. Therefore, the q and μ values of benzladehyde could not be accurately calculated. Nonetheless, it still can be stated that S-AP showed an ability to adsorb benzaldehyde, as the gas sampling bag with S-AP showed faster and greater reduction than the others. While it proved effective for higher aldehydes adsorption, S-AP was not effective for airborne acetone abatement (Figure 3d,

5573

dx.doi.org/10.1021/am400810s | ACS Appl. Mater. Interfaces 2013, 5, 5569–5577

initial acetone concentration was 94 ppm), under the conditions used. In fact, bare SBA-15 showed better adsorption of acetone than S-AP. This indicates that diffusion of acetone into the silica surface pores was efficient, but the reaction rate between the ketone and amine was much slower than for the aldehydes.

Adsorption Mechanism. The adsorption of aldehydes with aminosilica is driven by reaction between the carbonyl and the amine, and the reaction scheme is described elsewhere.[51−53] Though the previous literature discusses the reaction in solution in light of its use in organic synthesis, the same procedure can be proposed for airborne aldehyde/ketone capture,[15,33] although some changes may be possible because of the tethering of the amines to a surface, inhibiting the rotational and translation freedom that is found in solution. Scheme 1

Scheme 1. Reaction Scheme between an Aldehyde and an Amine during Aldehyde Adsorption
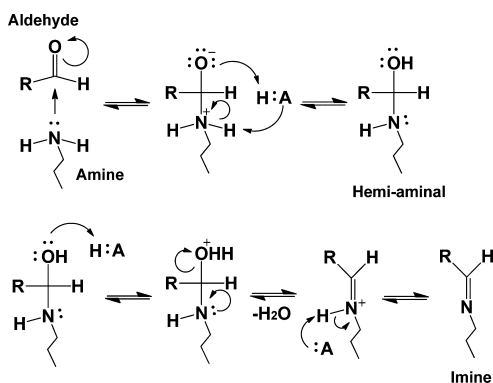
shows the possible reaction scheme of an aldehyde and a primary amine, in which the lone pair of amine nitrogen attacks the carbonyl carbon, and then undergoes proton exchange to form an unstable hemiaminal intermediate, and then finally the imine is formed by dehydration from the hemiaminal. The reaction steps are reversible reactions and the reaction is driven to the imine by removal of water. A secondary amine cannot form an imine because it does not have a proton available to be dehydrated from its hemiaminal; instead, hemiaminals from secondary amines often react further with another amine to form an aminal. In this case, two secondary amine molecules react with one aldehyde molecule, which likely explains the lowered efficiency, μ, of S-MAP compared to S-AP in all the aldehyde abatement tests in this study. Tertiary amines have no protons that can undergo hydrogen exchange and dehydration, and this is the likely reason why S-DMAP had no adsorption ability.

The reaction was initially verified by FT-Raman spectroscopy of S-AP samples after aldehyde VOC abatement tests (Figure 4). All the spectra in Figure 4 had a peak at 490 cm^{-1} that was assigned to the Si−O−Si vibration from the silica support, and S-AP spectrum before and after VOC adsorption showed strong peaks derived from the propyl chain, 2900 cm^{-1} for C−H stretching and 1450 cm^{-1} for CH_2 bending. In addition to these peaks, they also showed a strong Raman band at 1640 cm^{-1} on the acetaldehyde, hexanal, and benzaldehyde adsorbed S-AP samples, which were attributed to C=N stretching modes, signifying the formation of the imine species via reactive adsorption.[54] S-AP after benzaldehyde adsorption had additional peaks that are assigned to vibrations of phenyl group
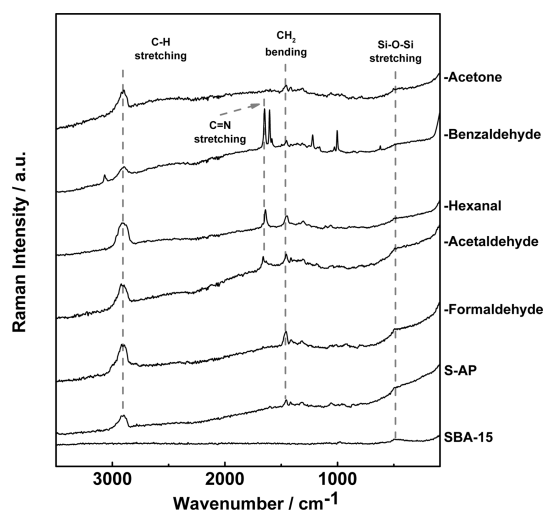

Figure 4. FT Raman spectra of pristine SBA-15 and S-AP (lower bottom two). FT Raman spectra of S-APs after abatement tests of formaldehyde, acetaldehyde, hexanal, benzaldehyde, and acetone gases are also depicted.

(3070, 1600, 1220, 1000 cm^{-1}), supporting that aldehydes are covalently attached to the amines on the silica surface. These peaks did not lose their intensities after remeasurement after one week of storage under an ambient atmosphere, indicating that the adsorbed aldehydes are stably trapped, even though the reaction (Scheme 1) is formally reversible. This evidence of stably captured aldehydes demonstrates an advantageous aspect of aminosilicas as airborne aldehyde abatement materials, as they show no significant leakage of aldehydes after adsorption under the conditions used.

Interestingly, the FT-Raman spectrum of the S-AP material after acetone and formaldehyde abatement tests did not show any significant changes from the original spectrum of fresh S-AP. A similar spectrum for S-AP before and after acetone abatement tests is quite reasonable, as we noted above that acetone was not efficiently captured by the material within the examined range of time. Acetone can potentially react with an amine following the same scheme as for aldehydes, but the reaction rate is much slower than with aldehydes due to the stabilized carbonyl carbon associated with two neighboring methyl groups. Thus, the lack of acetone capture with these materials, as verified by FT-Raman spectroscopy, can be rationalized.

In contrast, the observation of a FT-Raman spectrum for S-AP before and after formaldehyde adsorption was initially unexpected, as the S-AP material clearly reduced the airborne formaldehyde concentration. One difference in the tests is that for formaldehyde abatement tests, a much higher concentration of water (900 ppm) was added to the gas sampling bag during the injection of formaldehyde. We hypothesized this water may prohibit the elimination of water from the hemiaminal intermediate and prevent formation of the imine in Scheme 1.

NMR spectroscopy was therefore used to further confirm the reactions occurring during the aldehyde adsorption. Figure 5a presents the ^{13}C CP MAS solid-state NMR spectrum of S-AP that adsorbed airborne ^{13}C labeled formaldehyde (^{13}C-formaldehyde). The native formaldehyde carbon peak at 197 ppm completely disappeared, and instead, two intensive peaks at 75 and 153 ppm were observed, including a small shoulder peak at 85 ppm. The three minor peaks that also appear at 12, 23, and
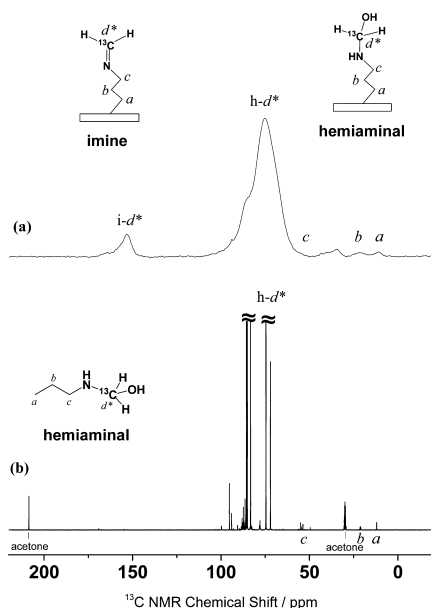
Figure 5. (a) ^{13}C CP MAS NMR spectrum for ^{13}C-formaldehyde adsorbed S-AP and (b) ^{13}C solution NMR spectrum for equimolar solution of ^{13}C-formaldehyde and propylamine in acetone-d_6. The h and i assigned on peaks denote carbons derived from hemiaminal and imine, respectively.

43 ppm are assigned to the carbons of the propyl group of S-AP.[37] The two intense peaks suggest that adsorbed formaldehyde was chemically attached to the amine surface and converted to hemiaminal (75 ppm) and imine (153 ppm) species. These ^{13}C NMR data do not quantitatively depict the hemiaminal and imine ratio derived from adsorption of ^{13}C-formaldehyde. However, it can be deduced that the captured formaldehyde species are dominantly in the hemiaminal state, as no imine structure was observed by Raman spectroscopy. Hemiaminals are often considered to be unstable compounds that are likely to be converted to the imine or the initial amine, but in this case, we hypothesize the species on the S-AP surface remained as a stable hemiaminal due to the humidity in the air. Although the Raman spectroscopic data (Figure 4) presented no evidence of the imine structure after formaldehyde adsorption, we could confirm by ^{13}C NMR that the imine was partially produced. Figure 5b shows the ^{13}C NMR of an equimolar solution of aqueous ^{13}C-formaldehyde and propylamine. Propylamine was used as a liquid phase model for the surface bound primary amine of the S-AP material. Formation of the hemiaminal was also observed in the solution phase, and the conversion from propylamine to the hemiaminal was ca. 44% from the ^1H NMR spectrum (see the Supporting Information). The imine structure was not found in the solution phase, which may be due to the excess of water that was contained in the formaldehyde solution. The other peaks around 83−95 ppm in Figure 5b are unreacted formaldehyde derivatives that are poly(acetals) or trioxane, and these peaks may appear in the solid state ^{13}C CP MAS NMR spectrum (Figure 5a) as a shoulder peak around 85 ppm. These observations indicate that some of the adsorbed formaldehyde is not reacted with amines, but rather adsorbs or deposits on the aminosilica surface in the poly(acetal) or trioxane states, and demonstrates another driving force for formaldehyde adsorption outside the amine-aldehyde chemical reaction.

The adsorption of acetaldehyde by S-AP was also monitored using ^{13}C labeled acetaldehyde ($^{13}C_2$-acetaldehyde). Figure 6a shows the ^{13}C CP MAS solid-state NMR spectrum of airborne $^{13}C_2$-acetaldehyde adsorbed on S-AP. Both of the carbon peaks derived from the hemiaminal ($^{13}CH_3$-$^{13}CHOH$-, 17 ppm; and $^{13}CH_3$-$^{13}CHOH$-, 50 ppm) and the imine ($^{13}CH_3$-^{13}CH=N-, 17 ppm and, $^{13}CH_3$-^{13}CH=N-, 163 ppm) structures were observed. The spectrum presented two new peaks at 143 and 132 ppm, which can be attributed to the carbons of an enamine that was tautomerized from the imine, as illustrated in Scheme 2.[55] ^{13}C NMR of an equimolar solution of $^{13}C_2$-acetaldehyde and propylamine (Figure 6b) also showed the formation of the imine, and its conversion from propylamine to the corresponding imine was estimated to be about 51% based on the ^1H NMR spectrum (see the Supporting Information). Traces of the hemiaminal structure of acetaldehyde-propylamine produce were observed (Figure 6b superimposed, the conversion to this hemiaminal could not be explicitly calculated). However, as opposed to the formaldehyde reaction, the imine was the dominant product even if excess water was added to the acetaldehyde-propylamine mixture. This is because the methyl group of acetaldehyde (phenyl group for benzaldehyde and pentyl group for hexanal) stabilized its imine structure. In the case of solution phase NMR, the enamine structure of acetaldehyde-propylamine reactant was not clearly observed, whereas solid-state NMR data suggested its existence. As the imine is more stable than the enamine in imine-enamine tautomarization equilibria, the reason why the enamine structure was clearly observed in the solid phase reactions is not clear. However, the enamine produced is a secondary amine, and this can further react with excess of airborne acetaldehyde, as with S-MAP silica. Such extended reaction pathways in the solid phase may thus present the enamine product in the solid phase NMR spectra. In any case, those NMR spectra verify the reaction shown in Scheme 1 for the acetaldehyde adsorption, as with formaldehyde, and those reactions are the driving force for airborne aldehyde adsorption by amine-functionalized silicas.

■ SUMMARY

We have investigated amine-functionalized mesoporous silica as an airborne aldehyde adsorbent material, and studied the adsorption mechanism. Mesoporous SBA-15 silica with high surface area and large porosity was functionalized by three aminosilanes to create three aminosilica adsorbents with primary, secondary, and tertiary amines. The primary aminosilica, S-AP, was the most effective aldehyde adsorbent, reducing the airborne formaldehyde concentration with an adsorption capacity (at 88 ppm initial aldehyde concentration) of 1.4 $mmol_{HCHO}$ g^{-1}. The same material also adsorbed significant amounts of acetaldehyde, hexanal, and benzaldehyde gases. Although the airborne aldehyde concentrations used here are approximately 1−2 orders of magnitude higher than those found in contaminated air streams, they promote large aldehyde loadings on the surface that facilitated detailed spectroscopic studies that were used to verify the adsorption mechanisms. High adsorption capacities were achieved because of the nature of the supported mesoporous silica samples, having high surface areas, pore volumes, and amine loadings. Commercially available porous silica with a lower surface area and pore volume than SBA-15 was also used as the aminosilica support, and the resulting aminosilica composite was also quite
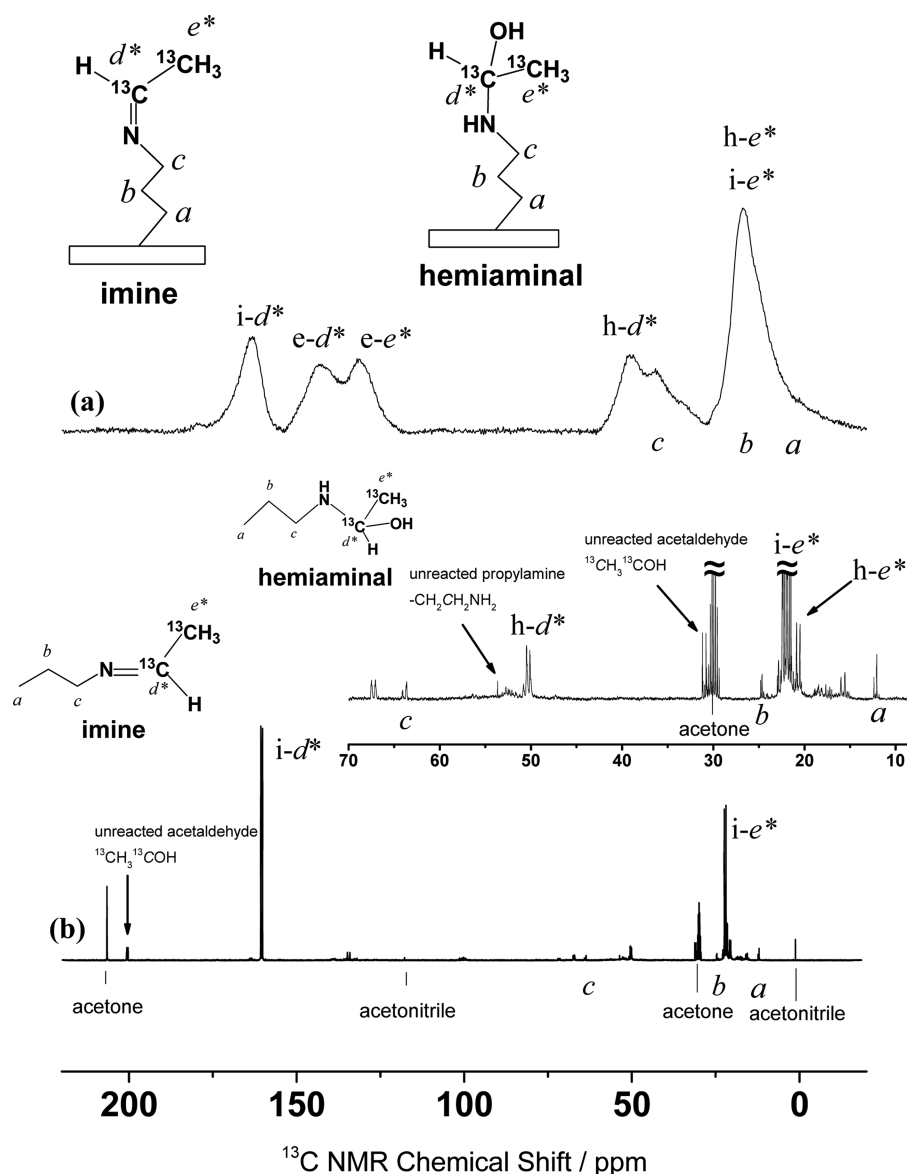
Figure 6. (a) ^{13}C CP MAS NMR spectrum for $^{13}C_2$-acetaldehyde adsorbed S-AP and (b) ^{13}C solution NMR spectrum for equimolar solution of $^{13}C_2$-acetaldehyde and propylamine in acetone-d_6. The h, i, and e assigned on peaks denote carbons derived from hemiaminal, imine, and enamine respectively. (b) The imine carbon peaks (i-d^* 160 ppm and i-e^* 22 ppm) had a coupling constant of 48 Hz between the neighboring ^{13}C nuclei. The hemiaminal carbon peaks (superimposed) (h-d^* 50 ppm and h-e^* 21 ppm) had a coupling constant of 37 Hz between the neighboring ^{13}C nuclei.

Scheme 2. Tautomerization between Imine and Enamine Structures
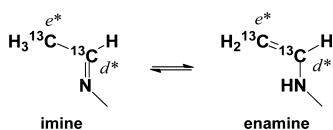
effective. The adsorption mechanism was studied by NMR and FT-Raman spectroscopy, to assess the products of the amine reaction with aldehydes, confirming the formation of imine and hemiaminal structures on the aminosilica surface after aldehyde adsorption. The generated imine to hemiaminal ratio depended on the presence or absence of water in the experimental system, but both forms effectively trapped airborne aldehydes stably on the aminosilica surface. As expected from this reaction scheme, the adsorption capacity and capturing efficiency decreased

when the secondary aminosilica was used, and the tertiary aminosilica was not effective for aldehyde adsorption. This work demonstrates the utility of amine-functionalized silica as efficient gaseous aldehyde adsorbents, depicts the aldehyde adsorption modes, and demonstrates that such materials hold promise as air purification materials by themselves or by incorporation into air purification materials such as filters or coatings.

■ ASSOCIATED CONTENT

Ⓢ Supporting Information

Chemical structures of the target VOCs for adsorptive abatement and ^{13}C labeled aldehydes in this study are shown in Figures S1 and S2, respectively. TGA data and nitrogen isotherms of functionalized silicas are shown in Figures S3 and S4, respectively. The results of formaldehyde abatement tests at 10 ppm initial concentration are shown in Figure S5. SEM

images of SBA-15 and PD09024 silicas are shown in Figure S6. ^{1}H NMR spectra of equimolar solutions of ^{13}C-formaldehyde-propylamine and $^{13}C_2$-acetaldehyde-propylamine in acetone-d_6 are shown in Figures S7 and S8, respectively. This information is available free of charge via the Internet at http://pubs.acs.org/.

■ AUTHOR INFORMATION

Corresponding Author
*E-mail: cjones@chbe.gatech.edu;.

Notes
The authors declare no competing financial interest.

■ REFERENCES

(1) Spengler, J. D.; Sexton, K. *Science* **1983**, *221*, 9−17.
(2) Tancrede, M.; Wilson, R.; Zeise, L.; Crouch, E. A. C. *Atmos. Environ.* **1987**, *21*, 2187−2205.
(3) Klepeis, N. E.; Nelson, W. C.; Ott, W. R.; Robinson, J. P.; Tsang, A. M.; Switzer, P.; Behar, J. V.; Hern, S. C.; Engelmann, W. H. *J. Expo. Anal. Environ. Epidemiol.* **2001**, *11*, 231−252.
(4) Harada, K.; Hasegawa, A.; Wei, C. N.; Minamoto, K.; Noguchi, Y.; Hara, K.; Matsushita, O.; Noda, K.; Ueda, A. *J. Health Sci.* **2010**, *56*, 488−501.
(5) Cogliano, V. J.; Grosse, Y.; Baan, R. A.; Straif, K.; Secretan, M. B.; El Ghissassi, F.; Working Grp, V. *Environ. Health Persp.* **2005**, *113*, 1205−1208.
(6) Mathew, T.; Suzuki, K.; Ikuta, Y.; Takahashi, N.; Shinjoh, H. *Chem. Commun.* **2012**, *48*, 10987−10989.
(7) Xu, J.; White, T.; Li, P.; He, C. H.; Han, Y. F. *J. Am. Chem. Soc.* **2010**, *132*, 13172−13173.
(8) Imamura, S.; Uematsu, Y.; Utani, K.; Ito, T. *Ind. Eng. Chem. Res.* **1991**, *30*, 18−21.
(9) Zhang, C.; He, H. *Catal. Today* **2007**, *126*, 345−350.
(10) Li, C. Y.; Shen, Y. N.; Jia, M.; Sheng, S. S.; Adebajo, M. O.; Zhu, H. Y. *Catal. Commun.* **2008**, *9*, 355−361.
(11) Qiu, X. Q.; Miyauchi, M.; Sunada, K.; Minoshima, M.; Liu, M.; Lu, Y.; Li, D.; Shimodaira, Y.; Hosogi, Y.; Kuroda, Y.; Hashimoto, K. *ACS Nano* **2012**, *6*, 1609−1618.
(12) Zhao, J.; Yang, X. D. *Build. Environ.* **2003**, *38*, 645−654.
(13) Hoffmann, M. R.; Martin, S. T.; Choi, W. Y.; Bahnemann, D. W. *Chem. Rev.* **1995**, *95*, 69−96.
(14) Fujishima, A.; Zhang, X. T.; Tryk, D. A. *Surf. Sci. Rep.* **2008**, *63*, 515−582.
(15) Zhu, Y. H.; Li, H.; Zheng, Q.; Xu, J. Q.; Li, X. X. *Langmuir* **2012**, *28*, 7843−7850.
(16) Gesser, H. D. U.S. Patent 4 547 350, Oct 15, 1985.
(17) Gesser, H. D.; Fu, S. L. *Environ. Sci. Technol.* **1990**, *24*, 495−497.
(18) Lee, Y. G.; Oh, C.; Kim, D. W.; Jun, Y. D.; Oh, S. G. *J. Ceram. Process. Res.* **2008**, *9*, 302−306.
(19) Strommen, M.; Gesser, H. D. *Cent. Eur. J. Chem* **2011**, *9*, 404−409.
(20) Gesser, H. D. U.S. Patent 4 892 719, Jan 9, 1990.
(21) Visioli, D. L.; Brodie, V., III. U.S. Patent 5 350 788, Sept 27, 1994.
(22) Brodie, V., III; Visioli, D. L. U.S. Patent 5 362 784, Nov 8, 1994.
(23) Brodie, V., III; Visioli, D. L. U.S. Patent 5 413 827, May 9, 1995.
(24) Koller, K. B.; Wrenn, S. E.; Houck Jr., W. G.; Paine, J. B., III. U.S. Patent 6 911 189B1, June 28, 2005.
(25) Khabbaz, F.; Eriksson, A. U.S. Patent 2006/0 222 877A1, March 30, 2006.
(26) Barrows, W.; Sirdeshpande, G.; Caldwell, K. G.; Garrick, J. R.; Cook, M. U.S. Patent 2010/0 016 152A1, July 20, 2009.
(27) Boyer, P.; Tutin, K.; Srinivasan, R. U.S. Patent 7 989 367B2, Aug 2, 2011.
(28) Tutin, K. K.; Gabrielson, K.; Rediger, R. U.S. Patent 8 043 383B2, Oct 25, 2011.
(29) Caldwell, K. G.; Sirdeshpande, G.; Barrows, W.; Garrick, J. R.; Cook, M. U.S. Patent 8 119 560B2, Feb 21, 2012.
(30) Green, G. D.; Swedo, R. J.; Tomlinson, I. A.; Whetten, A. R.; Coburn, C. E.; Henning, M. A.; Novy, P. M. U.S. Patent 8 236 263B2, Aug 7, 2012.
(31) Wu, S. U.S. Patent 2012/0 148 858A1, June 14, 2012.
(32) Tanada, S.; Kawasaki, N.; Nakamura, T.; Araki, M.; Isomura, M. *J. Colloid Interface Sci.* **1999**, *214*, 106−108.
(33) Sae-ung, S.; Boonamnuayvitaya, V. *Environ. Eng. Sci.* **2008**, *25*, 1477−1485.
(34) Bollini, P.; Brunelli, N. A.; Didas, S. A.; Jones, C. W. *Ind. Eng. Chem. Res.* **2012**, *51*, 15153−15162.
(35) Drese, J. H.; Talley, A. D.; Jones, C. W. *ChemSusChem* **2011**, *4*, 379−385.
(36) Ewlad-Ahmed, A. M.; Morris, M. A.; Patwardhan, S. V.; Gibson, L. T. *Environ. Sci. Technol.* **2012**, *46*, 13354−13360.
(37) Didas, S. A.; Kulkarni, A. R.; Sholl, D. S.; Jones, C. W. *ChemSusChem* **2012**, *5*, 2058−2064.
(38) Katiyar, A.; Ji, L.; Smirniotis, P.; Pinto, N. G. *J. Chromatogr. A* **2005**, *1069*, 119−126.
(39) Hicks, J. C.; Drese, J. H.; Fauth, D. J.; Gray, M. L.; Qi, G. G.; Jones, C. W. *J. Am. Chem. Soc.* **2008**, *130*, 2902−2903.
(40) Sing, K. S. W.; Everett, D. H.; Haul, R. A. W.; Moscou, L.; Pierotti, R. A.; Rouquerol, J.; Siemieniewska, T. *Pure Appl. Chem.* **1985**, *57*, 603−619.
(41) Lukens, W. W.; Schmidt-Winkel, P.; Zhao, D.; Feng, J.; Stucky, G. D. *Langmuir* **1999**, *15*, 5403−5409.
(42) Ping, E. W.; Wallace, R.; Pierson, J.; Fuller, T. F.; Jones, C. W. *Microporous Mesoporous Mater.* **2010**, *132*, 174−180.
(43) Wan, Y.; Zhao, D. Y. *Chem. Rev.* **2007**, *107*, 2821−2860.
(44) Heydari-Gorji, A.; Belmabkhout, Y.; Sayari, A. *Microporous Mesoporous Mater.* **2011**, *145*, 146−149.
(45) Ko, Y. G.; Shin, S. S.; Choi, U. S. *J. Colloid Interface Sci.* **2011**, *361*, 594−602.
(46) Sayari, A.; Belmabkhout, Y.; Da'na, E. *Langmuir* **2012**, *28*, 4241−4247.
(47) Trens, P.; Tanchoux, N.; Papineschi, P. M. *Colloid Surf. A-Physicochem. Eng. Asp.* **2011**, *381*, 92−98.
(48) Choi, S.; Drese, J. H.; Eisenberger, P. M.; Jones, C. W. *Environ. Sci. Technol.* **2011**, *45*, 2420−2427.
(49) Buszewski, B. *Chromatographia* **1992**, *34*, 573−580.
(50) Chudasama, V.; Fitzmaurice, R. J.; Caddick, S. *Nat. Chem.* **2010**, *2*, 592−596.
(51) Wagner, E. C. *J. Org. Chem.* **1954**, *19*, 1862−1881.
(52) Pine, S. H.; Sanchez, B. L. *J. Org. Chem.* **1971**, *36*, 829.
(53) Smith, B. M.; Jerry, M. *March's Advanced Organic Chemistry — Reactions, Mechanism, and Structures*, 6th ed.; Wiley, New York, 2007; pp 1281−1284.
(54) Socrates, G. *Infrared and Raman Characteristic Group Frequencies: Tables and Charts*, 3rd ed.; Wiley: New York, 2001.
(55) Lammertsma, K.; Prasad, B. V. *J. Am. Chem. Soc.* **1994**, *116*, 642−650.